Low oxidation state aluminum-containing cluster anions: Cp*AlnH−, n = 1–3

Xinxing Zhang, Gerd Ganteför, Bryan Eichhorn, Dennis Mayo, William H. Sawyer, Ann F. Gill, Anil K. Kandalam, Hansgeorg Schnöckel, and Kit Bowen

Citation: The Journal of Chemical Physics **145**, 074305 (2016); doi: 10.1063/1.4959847
View online: http://dx.doi.org/10.1063/1.4959847
View Table of Contents: http://scitation.aip.org/content/aip/journal/jcp/145/7?ver=pdfcov
Published by the AIP Publishing

Low oxidation state aluminum-containing cluster anions: $Cp^*Al_nH^-$, n = 1–3

Xinxing Zhang (张新星),[1] Gerd Ganteför,[1] Bryan Eichhorn,[2] Dennis Mayo,[3] William H. Sawyer,[4] Ann F. Gill,[4] Anil K. Kandalam,[4,a)] Hansgeorg Schnöckel,[5] and Kit Bowen[1,a)]

[1]*Department of Chemistry, Johns Hopkins University, Baltimore, Maryland 21218, USA*
[2]*Department of Chemistry, University of Maryland, College Park, Maryland 20742, USA*
[3]*EOD Technology Division, Naval Surface Warfare Center, Indian Head, Maryland 20640, USA*
[4]*Department of Physics, West Chester University of PA, West Chester, Pennsylvania 19383, USA*
[5]*Institute of Inorganic Chemistry, Karlsruhe Institute of Technology, D-76131 Karlsruhe, Germany*

(Received 11 May 2016; accepted 14 July 2016; published online 16 August 2016)

Three new, low oxidation state, aluminum-containing cluster anions, $Cp^*Al_nH^-$, n = 1–3, were prepared *via* reactions between aluminum hydride cluster anions, $Al_nH_m^-$, and Cp*H ligands. These were characterized by mass spectrometry, anion photoelectron spectroscopy, and density functional theory based calculations. Agreement between the experimentally and theoretically determined vertical detachment energies and adiabatic detachment energies validated the computed geometrical structures. Reactions between aluminum hydride cluster anions and ligands provide a new avenue for discovering low oxidation state, ligated aluminum clusters. *Published by AIP Publishing.* [http://dx.doi.org/10.1063/1.4959847]

INTRODUCTION

In the recent years, aluminum chemistry has experienced a renaissance as a result of increased interest in the reactivity of its low oxidation state compounds.[1,2] Since Schnöckel first synthesized metastable aluminum mono-halide solutions more than 30 years ago,[3,4] they have become the principle precursors from which a variety of ligated aluminum compounds have been synthesized.[1,2,5–13]

Among the ligand constituents of these compounds, Cp*, i.e., pentamethylcyclopentadienyl, has often played a starring role. The cluster, $(Cp^*Al)_4$, was an early example of a ligated aluminum compound synthesized by Schnöckel; it having been prepared through the reaction of an AlCl solution with Cp^*_2Mg.[11–13] $(Cp^*Al)_4$ has a unique chemistry, resulting from aluminum's +1 oxidation state.[14–23] Its versatility is illustrated by the fact that $(Cp^*Al)_4$ can react with the main group element compounds to form unusual cluster structures, such as rings and cages.[21–23] $(Cp^*Al)_4$ can also dissociate into monomeric Cp*Al units,[14] and since these have lone electron pairs on their aluminum sides, they can act as ligands in transition metal complexes.[16–20] Additionally, $[Cp^*AlH_2]_3$ and Cp^*_2AlH have been prepared. In the latter case, Cp^*_2AlH is in equilibrium with Cp*H and Cp*Al.[24] Cp* is also an important ligand in aluminum-rich metalloid clusters, such as $Al_{50}Cp^*_{12}$; this cluster having been prepared using the precursor, AlBr.[25] $(Cp^*Al)_4$ has also been used to make $Al_8Cp^*_4$.[26] Aluminum-rich clusters have received special attention because of their potential as energetic materials.[27] Other than these ligated clusters, the monovalency of Al in bare Al clusters was also discussed theoretically.[28]

In the present work, we extend the study of Cp*-ligated aluminum clusters into the gas phase. We report the formation and the anion photoelectron spectra of three previously unknown cluster anions: $Cp^*Al_nH^-$, n = 1–3. These were formed due to the reactions of aluminum hydride cluster anions $Al_nH_m^-$ with Cp*H in a beam-gas reaction cell. We also report density functional theory (DFT) based calculations which were used to identify the lowest energy structures of the neutral (^{0}) and negatively charged (−) $Cp^*Al_nH^{0/-}$ systems. Comparisons between the experimentally and theoretically determined vertical detachment energies (VDEs) and adiabatic detachment energies (ADEs) validated the computed geometrical structures.

METHODS

Experimental

Aluminum hydride cluster anions, $Al_nH_m^-$, were generated in a pulsed arc cluster ionization source (PACIS) which has been described in detail elsewhere.[29–32] This source has proven to be a powerful tool for generating metal hydrides and their anions.[30–37] Briefly, a ~30 μs duration, 150 V electric pulse was applied across an anode and a sample cathode, vaporizing aluminum atoms and forming a plasma. In the present case, the sample cathode was a 0.5 in. diameter pure aluminum rod. About 200 psi of ultrahigh purity hydrogen gas was also injected into the arc region through a pulsed valve. The hydrogen gas, which had been partially dissociated by the discharge, propelled the aluminum-hydrogen atom plasma mixture down a 3 cm long flow tube, where its constituents interacted and formed cluster anions.

Anions generated by this method then passed through a 5 mm-wide gap before entering the reaction cell. These cluster anions were not mass-selected. The reaction cell was

a)Authors to whom correspondence should be addressed. Electronic addresses: AKandalam@wcupa.edu and kbowen@jhu.edu

a 10 cm long, 1 cm diameter tube with 2 mm diameter apertures on each end. These apertures helped to maintain a suitable concentration of reactants in the cell and to minimize back-flow. To introduce Cp*H ligands into the reaction cell, 50 psi of Cp*H-seeded, ultra-high purity helium was injected through an aperture on the side of the reaction cell by a second pulsed valve. This aperture was mounted on the downstream end of the cell in order to reduce back-flow. The amount of Cp*H injected into the cell was controlled by varying the valve's pulse duration from 50 μs to 250 μs. The resulting anionic reaction products, along with unreacted $Al_nH_m^-$, continued to drift toward the extraction plates of the time-of-flight mass spectrometry portion of the apparatus, from where their mass spectra were recorded. Cluster anions of interest were then mass-selected and their photoelectron spectra recorded.

Anion photoelectron spectroscopy is conducted by crossing mass-selected, negative ions with fixed-energy photons and analyzing the energies of the resultant photodetached electrons. This technique is governed by the well-known energy-conserving relationship, hν = EBE + EKE, where hν, EBE, and EKE are the photon energy, electron binding energy (photodetachment transition energy), and the electron kinetic energy, respectively.

Our photoelectron apparatus, which has been described elsewhere,[38] consists of several possible anion sources, a linear time-of-flight mass spectrometer, a mass gate, a momentum decelerator, a neodymium-doped yttrium aluminum garnet (Nd:YAG) laser operated in the third harmonic (355 nm) for photodetachment, and a magnetic bottle electron energy analyzer with a resolution of 35 meV at EKE = 1 eV. The photoelectron spectra were calibrated against the well-known photoelectron spectrum of Cu^-.[39]

THEORETICAL

The lowest energy structures of neutral and negatively charged $Cp^*Al_nH^{0/-}$ (n = 1–3) systems were obtained by conducting density functional theory (DFT) based electronic structure calculations. The gradient-corrected Becke's exchange functional[40] combined with the Perdew-Wang correlation[41] functional (BPW91) and a 6-311+G** basis set were used for all the calculations; these being carried out using the Gaussian 09 software package.[42] Structural configurations of neutral and anionic $Cp^*Al_{1-3}H^{0/-}$ systems were optimized without symmetry constraints. In the geometry optimization procedure, the energy convergence criterion was set to 10^{-9} hartree, while the gradient was converged to 10^{-4} hartree/Å. The reliability and accuracy of the functional form used in this study to predict the lowest energy structures of metal organic systems was established in our earlier studies on metal-organic complexes.[43–47]

The vertical detachment energies (VDEs) and the higher energy transitions obtained from the theoretical calculations were compared with the corresponding measured values. The vertical detachment energy (VDE) is the energy difference between the ground state anion and its corresponding neutral in the geometry of the anion. The calculated adiabatic detachment energies (ADEs) of the lowest energy isomers of the cluster anions were compared to the onset (lowest electron binding energy) region of the anion photoelectron spectrum. The ADE is calculated as the energy difference between the lowest energy geometry of the anionic cluster and the structurally similar/identical isomer (nearest local minimum) of its neutral counterpart.

RESULTS AND DISCUSSION

Figures 1(a) and 1(b), respectively, present anion mass spectra before and after reaction. In Figure 1(a), several homologous aluminum hydride cluster anion, $Al_nH_m^-$, series are observed, i.e., those based on n = 2-8. After injecting Cp*H seeded in helium into the reaction cell, we observed the mass spectrum presented in Figure 1(b). There, residual intensities of unreacted aluminum hydride cluster anions share the spectrum with three higher intensity $Cp^*Al_nH^-$, n = 1-3 product peaks. Unit mass resolution was attained for all species in both spectra.

In Figures 2(a)–2(c), we present the anion photoelectron spectra of $Cp^*Al_1H^-$, $Cp^*Al_2H^-$, and $Cp^*Al_3H^-$, respectively. All three photoelectron spectra were measured with 3.49 eV photons. The EBE value corresponding to the intensity maximum in the lowest EBE spectral band is the vertical detachment energy (VDE). The VDE is the photodetachment transition energy at which the Franck-Condon overlap between the wave functions of the anion and its neutral counterpart is maximal. The electron affinity (EA) is the energy difference between the lowest energy state of the anion and the lowest energy state of its neutral counterpart. When significant Franck-Condon overlap exists between $v = 0$ of the anion and $v' = 0$ of its corresponding neutral (the origin transition), and when no vibrational hot bands (photoelectrons from vibrationally excited anions) are present, the EA value corresponds to the EBE value at the intensity threshold of the lowest EBE band. Here, we have assigned EA values by extrapolating the low EBE side of the lowest EBE bands to

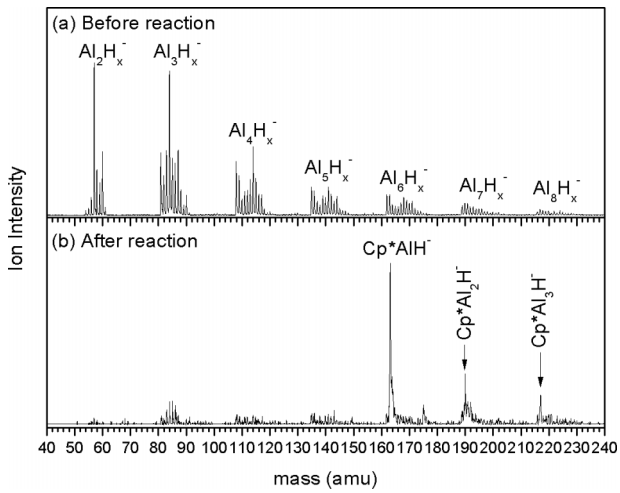

FIG. 1. (a) Mass spectrum of aluminum hydride cluster anions before reaction and (b) mass spectrum of $Cp^*Al_{1-3}H^-$ cluster anions after reaction.

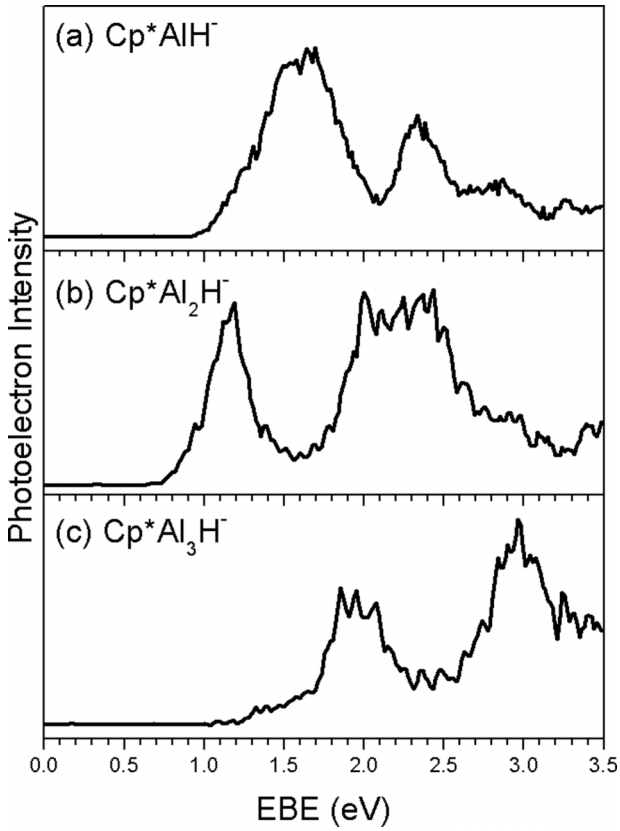

FIG. 2. Photoelectron spectra of $Cp^*Al_nH^-$ anions recorded with 3.49 eV photons: (a) n = 1, (b) n = 2, and (c) n = 3.

zero. All the experimental and theoretical VDE and ADE/EA values are tabulated in Table I.

The photoelectron spectrum of Cp^*AlH^- [see Figure 2(a)] exhibits a broad band between EBE = 1.0 and 2.0 eV, followed by several weaker peaks at higher EBE values. The EA of Cp*AlH is estimated from the spectrum to be 1.0 ± 0.2 eV, while the VDE of Cp^*AlH^- is seen to be 1.6 ± 0.1 eV. The calculated ground state geometric structure of anionic Cp^*AlH^- is shown in Figure 3(a). The aluminum atom binds to two carbon atoms (η^2 coordination) in the Cp* ring with an average Al–C bond length of 2.41 Å, while the hydrogen atom binds radially with the aluminum atom with an Al–H bond length of 1.75 Å. The calculated VDE of this anionic structure is 1.60 eV which is in good agreement with the measured value of 1.6 ± 0.1 eV. The HOMO of the anion from which the electron was photo-detached corresponds to an anti-bonding orbital between Al and H atoms. In the case of the ground state of neutral Cp*AlH, the aluminum atom

TABLE I. Experimentally determined EA and VDE values together with computationally determined ADE and VDE values. Computational results from different isomers are separated by a slash. All values are reported in eV.

	ADE/EA		VDE	
Species	Theoretical	Expt.	Theoretical	Expt.
Cp^*AlH/Cp^*AlH^-	0.85	1.0	1.60	1.6
$Cp^*Al_2H/Cp^*Al_2H^-$	0.73	0.8	1.04/0.85/1.20	1.2
$Cp^*Al_3H/Cp^*Al_3H^-$	1.20/1.00	1.2	1.40/1.20	1.4

prefers to bind to all five carbon atoms (η^5 coordination) of the Cp* ring [see Figure 3(b)], with an average Al–C bond length of 2.38 Å. The calculated ADE value of Cp*AlH is 0.85 eV which is in reasonable agreement with the measured value. The difference between ADE/EA and VDE values for this cluster is due to the structural difference between the anion and its neutral counterpart. The natural population analysis (NPA) charge analysis of the lowest energy structure of neutral Cp*AlH has revealed that there is a significant charge transfer from Al atom to the Cp* ligand and H atom, thereby resulting in a charge of +0.89*e* on the Al atom (see Fig. 3(b)). In the case of the anionic Cp^*AlH^- on the other hand, the NPA charge on Al atom is +0.30*e* (see Fig. 3(a)), showing that about 60% of the extra-electron's charge was localized on the Al ion.

The photoelectron spectrum of $Cp^*Al_2H^-$ [see Figure 2(b)] exhibits a band between EBE = 0.8 and 1.4 eV, followed by a broader band between EBE = 1.7 and ~3.0 eV. The VDE value of the $Cp^*Al_2H^-$ is 1.2 ± 0.1 eV. Our calculations show that there are three nearly degenerate (within 0.30 eV) structures for the doublet anionic $Cp^*Al_2H^-$ system [see Figs. 4(a)–4(c)]. Dimerization of the aluminum atoms, i.e., the formation of a metal-metal bond, is the common structural feature among these three isomers. Moreover, only one of the aluminum atoms in each case interacts directly with the Cp* ring. In the lowest energy anionic isomer [see Figure 4(a)], the proximal aluminum atom exhibits η^4 coordination with the Cp* ring. The next two higher energy anionic isomers display η^5 coordination [see Figure 4(b)] and η^2 coordination [see Figure 4(c)], respectively. Another notable structural difference among these isomers is the interaction of the hydrogen atom with the Al_2 dimeric moiety. In the lowest energy isomer [see Figure 4(a)], the hydrogen atom is weakly bound (based on bond lengths) to both the terminal aluminum atom and the proximal aluminum atom. In the next higher energy anionic isomer [see Figure 4(b)],

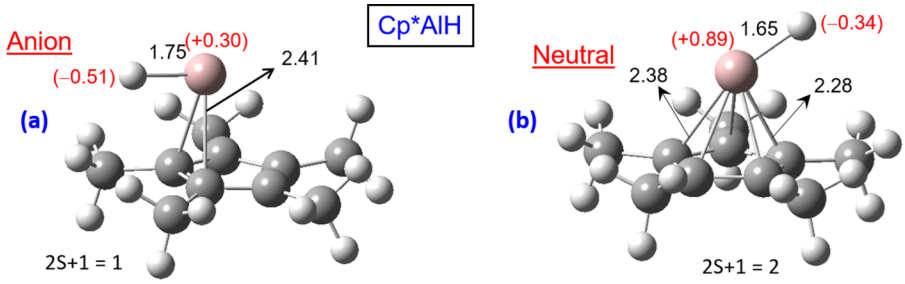

FIG. 3. Calculated structures of anionic and neutral $Cp^*Al_1H^{-/0}$ species. The NPA charges are given in parentheses. Also shown are their multiplicities and selected bond lengths (in Å).

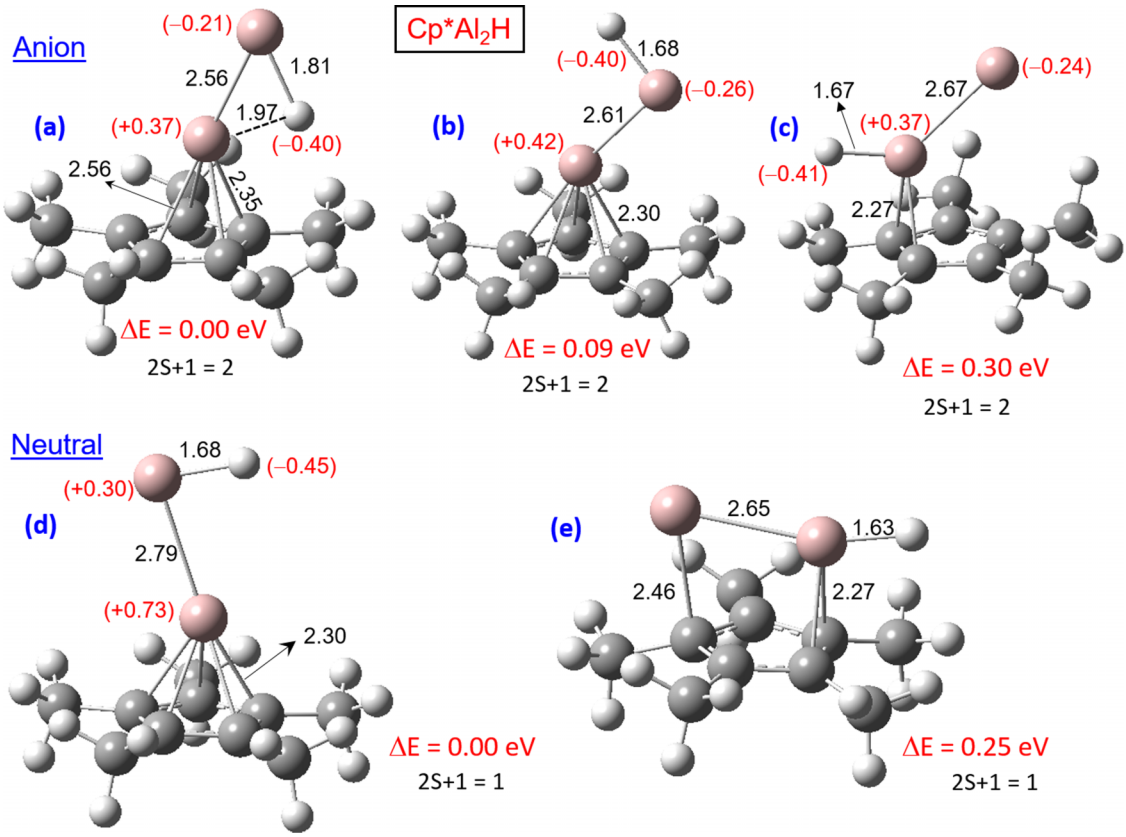

FIG. 4. Calculated structures of anionic and neutral $Cp^*Al_2H^{-/0}$ isomers. The NPA charges are given in parentheses. Also shown are their multiplicities, their relative energies (in eV), and selected bond lengths (in Å).

the hydrogen atom is relatively strongly bound to the terminal aluminum atom. In the highest energy anionic isomer [see Figure 4(c)], the hydrogen atom is also relatively strongly bound but only to the proximal aluminum atom. Since, the energy differences between these three isomers are small, we have calculated the vertical detachment energies for all three isomers. The calculated VDE values of the first anionic isomer [Figure 4(a)], the second isomer [Figure 4(b)], and the third isomer [Figure 4(e)] of $Cp^*Al_2H^-$ are 1.04 eV, 0.85 eV, and 1.20 eV, respectively. Note that all of these electron detachment energies correspond to transitions from anionic doublets to neutral singlet states. The lowest energy band in the photoelectron spectrum of $Cp^*Al_2H^-$ may be due to the overlap of peaks centered at 0.85 eV, 1.04 eV, and 1.20 eV, suggesting the presence of all three anionic isomers in the beam. Additionally, the calculated electron detachment energies for the anionic doublet to neutral triplet transitions occur at 2.54 eV, 1.78 eV, and 1.95 eV for the three isomers seen in Figures 4(a)–4(c), respectively. These lie under the higher EBE band in the photoelectron spectrum of $Cp^*Al_2H^-$.

For neutral Cp^*Al_2H, our calculations revealed two distinct structures, and these are shown in Figures 4(d) and 4(e). The lowest energy structure [see Figure 4(d)] consists of an aluminum dimeric moiety with one of its aluminum atoms interacting directly with the Cp* ring *via* η^5 coordination, while the hydrogen atom is bound to the terminal aluminum atom. This isomer is similar in structure to that of the second lowest energy anionic isomer [see Figure 4(b)]. In the higher energy neutral isomer [see Figure 4(e)], however, both aluminum atoms in the aluminum dimeric moiety interact with the Cp* ring, while the hydrogen atom is bound to one of the aluminum atoms. Interestingly, the structure of the lowest energy isomer of the anion [see Figure 4(a)] does not appear among the structures of neutral Cp^*Al_2H. The calculated ADE value for $Cp^*Al_2H^-$ is 0.73 eV which is in good agreement with the measured EA value of 0.8 ± 0.2 eV.

We now turn to the NPA charge analysis in the neutral and anionic Cp^*Al_2H. The charge distribution of the lowest energy isomer of neutral Cp^*Al_2H [see Fig. 4(d)] shows a total charge transfer of $-1.03e$ from the Al_2 moiety to Cp* ligand and H atom, with the proximal Al atom contributing 73% of this charge transfer. Note that this charge transfer is larger than that discussed in the Cp*AlH complex. A comparison of the charge distributions between the anionic [Figs. 4(a) and 4(b)] and neutral isomer [Fig. 4(d)] reveals that during the photodetachment process from the anionic $Cp^*Al_2H^-$, 87% of the electron's charge comes from the Al_2 moiety, with the terminal Al atom contributing 50% of this charge.

The photoelectron spectrum of anionic $Cp^*Al_3H^-$ [see Figure 2(c)] exhibits a spectral shoulder between EBE = 1.3 and 1.7 eV, followed by two well-defined bands, occurring between EBE = 1.7 eV and 2.3 eV and between EBE = 2.6 eV and 3.3 eV. The shoulder appears to be distinct from the first, well-defined band centered at EBE = 1.9 eV. As such,

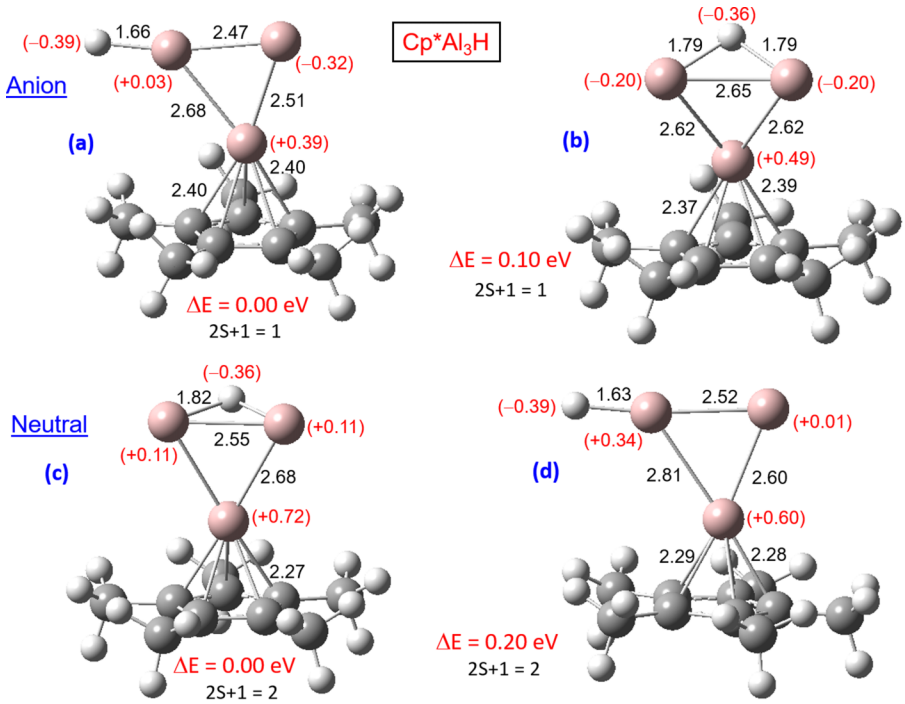

FIG. 5. Calculated structures of anionic and neutral $Cp^*Al_3H^{-/0}$ isomers. The NPA charges are given in parentheses. Also shown are their multiplicities, their relative energies (in eV), and selected bond lengths (in Å).

the shoulder represents the lowest EBE transitions in the spectrum. Based on this assumption, we assign the VDE value as 1.4 ± 0.2 eV and the EA value as 1.2 ± 0.2 eV.

The calculated structures of the two lowest energy isomers of anionic $Cp^*Al_3H^-$ are shown in Figures 5(a) and 5(b). In both of these nearly isoenergetic structural isomers, aluminum atoms bond as triangular, trimeric moieties with only one of their aluminum atoms interacting with the Cp* ring (*via* η^5 coordination). As in the anionic $Cp^*Al_2H^-$ case, these two isomers differ only in how their hydrogen atoms are bound to the aluminum trimeric moiety. In the case of the lowest energy anionic isomer [see Figure 5(a)], the hydrogen atom is terminally bound to one of the aluminum atoms, while in the other anionic isomer [see Figure 5(b)], the hydrogen atom bridges between two aluminum atoms. The calculated VDE value of the lowest energy isomer is 1.40 eV, which corresponds to the electron detachment from the HOMO that is dominated by bonding characteristic between the Al atoms of the Al_3 moiety. The VDE value of the higher energy isomer is 1.20 eV which again is due to the electron detachment from the bonding (between Al atoms) HOMO orbital. These values are in accord with the estimated experimental value of 1.4 eV. In addition, the calculated higher transition energies of EBE = 2.40 eV and 3.22 eV for the lowest energy anionic isomer and EBE = 2.71 and 3.72 eV for the other isomer may be contributing to the higher EBE bands of the photoelectron spectrum.

Interestingly, the structure of the lowest energy isomer of the neutral Cp^*Al_3H system [see Figure 5(c)] is similar to that of the anionic $Cp^*Al_3H^-$ isomer seen in Figure 5(b), while the structure of the lowest energy isomer of anionic $Cp^*Al_3H^-$ [see Figure 5(a)] is similar to that of the neutral Cp^*Al_3H isomer seen in Figure 5(d). The calculated adiabatic detachment energies (ADEs) of $Cp^*Al_3H^-$ are 1.20 eV for the lowest energy isomer [see Figure 5(a)] and 1.00 eV for the slightly higher energy isomer [see Figure 5(b)]. These ADE values compare reasonably well with the estimated EA value of 1.2 ± 0.2 eV. The NPA charge analysis of the two isomers of neutral Cp^*Al_3H [Figs. 5(c) and 5(d)] also reveal a similar picture as the neutral Cp^*Al_2H, namely a significant amount of charge transfer from the Al moiety to its ligands. In both of the neutral isomers, a total charge transfer of $-0.94e$ from the Al_3 moiety to Cp* ligand and H, with the proximal Al atom contributing majority of that charge transfer [72% in lowest isomer and 60% in the higher energy isomer]. A comparison of the charge distributions in the anionic and neutral isomers of Cp^*Al_3H again reveals a familiar picture. During the photodetachment of the electron from the anionic $Cp^*Al_3H^-$, 85% of the electron's charge is lost by the Al_3 moiety, while the remaining 15% of the electron's charge is contributed by the Cp* ligand. Lastly, in $Cp^*Al_nH^-$ species with $n > 1$, only a single aluminum atom interacts with the π-complex's structure. In addition, there is no clear preference between bridged-hydrogen and terminal hydrogen-containing structures.

For aluminum, any oxidation states (OS) other than +3 and 0 are considered to be low OS. In this study, the (average) OS of aluminum in the three clusters, $Cp^*Al_nH^-$ are +1, +1/2, and +1/3 for n = 1, 2, 3, respectively, given the conventional wisdom that the OS of Cp* and H are both −1. The low oxidation states of aluminum in the mono-ligated Cp^*Al_nH aluminum clusters studied here make them not only perspective reactive reagents for synthetic applications but also potential components of energetic materials.

ACKNOWLEDGMENTS

The experimental part of this material is based upon work supported by the Air Force Office of Scientific Research (AFOSR) under Grant No. FA9550-15-1-0259 (K.H.B.). The

computational portion of this work was supported by the WCUPA College of Arts and Sciences, Student Engagement Grant (A.K.K.).

[1]H. W. Roesky and S. S. Kumar, Chem. Commun. **2005**, 4027.
[2]H. W. Roesky, Inorg. Chem. **43**, 7284 (2004).
[3]H. Schnöckel, Z. Naturforsch., B: J. Chem. Sci. **31**, 1291 (1976).
[4]M. Tacke and H. Schnöckel, Inorg. Chem. **28**, 2896 (1989).
[5]R. Purath, R. Köppe, and H. Schnöckel, Angew. Chem. **111**, 3114 (1999); Angew. Chem., Int. Ed. **38**, 2926 (1999).
[6]A. Purath, R. Köppe, and H. Schnöckel, Chem. Commun. **1999**, 1933.
[7]H. Köhnlein, A. Purath, C. Klemp, E. Baum, I. Krossing, G. Stösser, and H. Schnöckel, Inorg. Chem. **40**, 4830 (2001).
[8]C. Dohmeier, M. Mocker, H. Schnöckel, A. Lötz, U. Schneider, and R. Ahlrichs, Angew. Chem. **105**, 1491 (1993); Angew.Chem., Int. Ed. Engl. **32**, 1428 (1993).
[9]A. Schnepf and H. Schnöckel, Adv. Organomet. Chem. **47**, 235 (2001).
[10]C. Üffing, A. Ecker, R. Köppe, K. Merzweiler, and H. Schnöckel, Chem. Eur. J. **4**, 2142 (1998).
[11]C. Dohmeier, C. Roble, M. Tacke, and H. Schnöckel, Angew. Chem. **103**, 594 (1991).
[12]C. Dohmeier, D. Loos, and H. Schnöckel, Angew. Chem. **108**, 141 (1996).
[13]J. Gauss, U. Schneider, R. Ahlrichs, C. Dohmeier, and H. Schnöckel, J. Am. Chem. Soc. **115**, 2402 (1993).
[14]A. Haaland, K.-G. Martinsen, S. A. Shlykov, H. V. Volden, C. Dohmeier, and H. Schnöckel, Organometallics **14**, 3116 (1995).
[15]J. D. Gorden, A. Voigt, C. L. B. Macdonald, J. S. Silverman, and A. H. Cowley, J. Am. Chem. Soc. **122**, 950 (2000).
[16]C. Dohmeier, H. Krautscheid, and H. Schnöckel, Angew. Chem. **106**, 2570 (1994).
[17]C. Üffing, A. Ecker, R. Köppe, and H. Schnöckel, Organometallics **17**, 2373 (1998).
[18]Q. Yu, A. Purat, A. Douchev, and H. Schnöckel, J. Organomet. Chem. **584**, 94 (1999).
[19]J. Weiß, D. Stetzkamp, B. Nuber, R. A. Fischer, C. Boehme, and G. Frenking, Angew. Chem., Int. Ed. Engl. **36**, 70 (1997).
[20]D. Weiß, T. Steinke, M. Winter, R. A. Fischer, N. Fröhlich, J. Uddin, and G. Frenking, Organometallics **19**, 4583 (2000).
[21]S. Schulz, T. Schoop, H. W. Roesky, L. Häming, A. Steiner, and R. Herbst-Irmer, Angew. Chem., Int. Ed. Engl. **34**, 919 (1995).
[22]C. K. F. von Haenish, C. Üffing, M. A. Junker, A. Ecker, B. O. Kneisel, and H. Schnöckel, Angew. Chem., Int. Ed. Engl. **35**, 2875 (1996).
[23]C. Dohmeier, H. Schnöckel, C. Robl, U. Schneider, and R. Ahlrichs, Angew. Chem., Int. Ed. Engl. **33**, 199 (1994).
[24]C. Ganesamoorthy, S. Loerke, C. Gemel, P. Jerabek, M. Winter, G. Frenking, and R. A. Fischer, Chem. Commun. **49**, 28580 (2013).
[25]J. Vollet, J. R. Hartig, and H. Schnöckel, Angew. Chem. Int. Ed. **43**, 3186 (2004).
[26]K. Weiß and H. Schnpckel, Anal. Bioanal. Chem. **377**, 1098 (2003).
[27]K. S. Williams and J. P. Hooper, J. Phys. Chem. A **115**, 14100 (2011).
[28]B. K. Rao and P. Jena, J. Chem. Phys. **111**, 1890 (1999).
[29]X. Zhang, Y. Wang, H. Wang, A. Lim, G. Gantefoer, K. H. Bowen, J. U. Reveles, and S. N. Khanna, J. Am. Chem. Soc. **135**, 4856 (2013).
[30]X. Li, A. Grubisic, S. T. Stokes, J. Cordes, G. F. Gantefoer, K. H. Bowen, B. Kiran, M. Willis, P. Jena, R. Burgert, and H. Schnoeckel, Science **315**, 356 (2007).
[31]X. Zhang, H. Wang, E. Collins, A. Lim, G. Ganteför, B. Kiran, H. Schnöckel, B. Eichhorn, and K. H. Bowen, J. Chem. Phys. **138**, 124303 (2013).
[32]J. D. Graham, A. M. Buytendyk, X. Zhang, E. L. Collins, K. Boggavarapu, G. Gantefoer, B. W. Eichhorn, G. L. Gutsev, S. Behera, P. Jena, and K. H. Bowen, J. Phys. Chem. A **118**, 8158 (2014).
[33]X. Zhang, G. Liu, G. Gantefoer, K. H. Bowen, and A. N. Alexandrova, J. Phys. Chem. Lett. **5**, 1596 (2014).
[34]X. Zhang, P. Robinson, G. Gantefoer, A. Alexandrova, and K. H. Bowen, J. Chem. Phys. **143**, 094307 (2015).
[35]A. Buytendyk, J. Graham, H. Wang, X. Zhang, E. Collins, Y. J. Ko, G. Gantefoer, B. Eichhorn, A. Regmi, K. Boggavarapu, and K. H. Bowen, Int. J. Mass Spectrom. **365-366**, 140 (2014).
[36]H. Wang, X. Zhang, Y. Ko, G. F. Gantefor, K. H. Bowen, X. Li, K. Boggavarapu, and A. Kandalam, J. Chem. Phys. **140**, 164317 (2014).
[37]X. Zhang, H. Wang, G. Ganteför, B. W. Eichhorn, and K. H. Bowen, Int. J. Mass Spectrom. **404**, 24–28 (2016).
[38]M. Gerhards, O. C. Thomas, J. M. Nilles, W. J. Zheng, and K. H. Bowen, J. Chem. Phys. **116**, 10247 (2002).
[39]J. Ho, K. M. Ervin, and W. C. Lineberger, J. Chem. Phys. **93**, 6987 (1990).
[40]A. D. Becke, Phys. Rev. A **38**, 3098 (1988).
[41]J. P. Perdew and Y. Wang, Phys. Rev. B **45**, 13244 (1992).
[42]M. J. Frisch, G. W. Trucks, H. B. Schlegel *et al.*, GAUSSIAN 09, Revision D.01, Gaussian, Inc., Wallingford, CT, 2004.
[43]A. K. Kandalam, B. K. Rao, and P. Jena, J. Chem. Phys. **120**, 10414 (2004).
[44]A. K. Kandalam, B. K. Rao, and P. Jena, J. Phys. Chem. A **109**(41), 9220 (2005).
[45]A. K. Kandalam, B. Kiran, P. Jena, X. Li, A. Grubisic, and K. H. Bowen, J. Chem. Phys. **126**, 084306 (2007).
[46]A. K. Kandalam, P. Jena, X. Li, S. N. Eustis, and K. H. Bowen, J. Chem. Phys. **129**, 134308 (2008).
[47]X. Li, S. Eustis, K. H. Bowen, A. K. Kandalam, and P. Jena, J. Chem. Phys. **129**, 074313 (2008).